molecular
systems
biology

Adaptation by stochastic switching of a monostable genetic circuit in *Escherichia coli*

Saburo Tsuru[1], Nao Yasuda[2], Yoshie Murakami[1], Junya Ushioda[1], Akiko Kashiwagi[3], Shingo Suzuki[1], Kotaro Mori[2], Bei-Wen Ying[1] and Tetsuya Yomo[1,2,4,*]

[1] Department of Bioinformatic Engineering, Graduate School of Information Science and Technology, Osaka University, Osaka, Japan, [2] Graduate School of Frontier Biosciences, Osaka University, Osaka, Japan, [3] Faculty of Agriculture and Life Science, Hirosaki University, Aomori, Japan and [4] Exploratory Research for Advanced Technology (ERATO), Japan Science and Technology Agency (JST), Osaka, Japan
* Corresponding author. Graduate School of Information Science and Technology, Osaka University, 1-5 Yamadaoka, Suita, Osaka 565-0871, Japan.
Tel.: +81 6 6879 4171; Fax: +81 6 6879 7433; E-mail: yomo@ist.osaka-u.ac.jp

Stochastic switching is considered as a cost-saving strategy for adaptation to environmental challenges. We show here that stochastic switching of a monostable circuit can mediate the adaptation of the engineered *OSU12-hisC Escherichia coli* strain to histidine starvation. In this strain, the *hisC* gene was deleted from the *His* operon and placed under the control of a monostable foreign promoter. In response to histidine depletion, the *OSU12-hisC* population shifted to a higher HisC expression level, which is beneficial under starving conditions but is not favoured by the monostable circuit. The population shift was accompanied by growth recovery and was reversible upon histidine addition. A weak directionality in stochastic switching of *hisC* was observed in growing microcolonies under histidine-free conditions. Directionality and fate decision were in part dependent on the initial cellular status. Finally, microarray analysis indicated that *OSU12-hisC* reorganized its transcriptome to reach the appropriate physiological state upon starvation. These findings suggest that bacteria do not necessarily need to evolve signalling mechanisms to control gene expression appropriately, even for essential genes.
Molecular Systems Biology **7**: 493; published online 24 May 2011; doi:10.1038/msb.2011.24
Subject Categories: signal transduction; microbiology and pathogens
Keywords: adaptation; gene regulation; monostability; stochastic switching; transciptome

Introduction

The fundamental mechanisms underlying adaptations can be divided into responsive switching and stochastic switching (Kussell and Leibler, 2005). Responsive switching is generally considered as resulting from evolved regulatory units, such as operons and regulons, which enable immediate adaptation (Jacob and Monod, 1961; Henkin and Yanofsky, 2002; Gama-Castro *et al*, 2008). However, as cells are subject to a wide range of both genetic and environmental perturbations that damage the specificity or efficiency of regulatory systems (Carroll, 2005; Crombach and Hogeweg, 2008), the limited number of regulatory units that can evolve and remain functional may not be sufficient to completely protect cell populations from the danger of extinction. Whether and how cells are able to survive external perturbations, when the corresponding regulatory units are absent or have been genetically disrupted, is an open question of great importance.

The studies on persistence, competence and sustenance proposed a complementary mechanism relying on stochastic switching (Balaban *et al*, 2004; Kussell and Leibler, 2005; Suel *et al*, 2007; Acar *et al*, 2008). Through a so-called 'bet-hedging' strategy, stochastic switching generates population diversity without the need for a specific responsive regulatory system (Slatkin, 1974). Noise in gene expression causes cell-to-cell variation and provides a chance for survival of the cells that occasionally are in the fit state (Avery, 2006). As stochastic switching requires neither an evolved regulatory unit nor the maintenance of any signal transduction machinery, it is considered as a universal cost-saving strategy for adaptation. Such stochastic switching-mediated survival strategy was greatly supported by the studies employing cells whose default sensing system was deficient or missing (Kashiwagi *et al*, 2006; Stolovicki *et al*, 2006; Suzuki *et al*, 2006; Stern *et al*, 2007; Isalan *et al*, 2008).

So far, the experimental evidence on stochastic switching was generally based on a bistable genetic structure (Kussell and Leibler, 2005; Kashiwagi *et al*, 2006; Stolovicki *et al*, 2006; Stern *et al*, 2007; Acar *et al*, 2008). Bistability allows the cells to stay at a stable state, either fit or unfit, so that the stochastically appearing

fit state can be stabilized without further random switching to the unfit state (Supplementary Figure S1; Kussell and Leibler, 2005; Acar *et al*, 2008). Owing to the fixation effect of bistability, the stochastic switching-induced population transition was intensively characterized (Kussell and Leibler, 2005; Acar *et al*, 2008). Nevertheless, the universality of stochastic switching as an adaptation strategy remains open, as bistability is known to be a special case in native genetic structures.

In contrast to bistable gene expression, monostable gene expression is much more common (Newman *et al*, 2006) and does not rely on a specific complex genetic architecture. Stochastic switching based on a monostable genetic structure has, however, not yet been identified as an accessible strategy for adaptation. Since a monostable structure has no fixation effect, the fit cells that appear stochastically tend to return to the original steady state (i.e., unfit state) (Supplementary Figure S1). To achieve a population shift from a maladaptive state (but stable) to an adaptive state (but unstable), a significant increase in fitness (i.e., growth rate) of the fit cells is necessary. Otherwise, the random switching will mask occasionally occurring adaptive transitions and lead to an unchanged population at the stable but maladaptive state. Therefore, in contrast to a bistable structure, the final adaptive state in a monostable system is not determined *a priori* by the genetic architecture, but is determined by the cellular response.

Whether adaptation can be achieved by stochastic switching based on a monostable structure is an intriguing issue. To address this question, we used an engineered *Escherichia coli* strain carrying a monostable genetic circuit that allows the experimental observation on stochastic switching. In this strain, the gene *hisC* was deleted from the *His* operon and placed under the control of a foreign gene circuit at another chromosomal locus, as previously described (Kashiwagi *et al*, 2009). The circuit showed a clear monostable behaviour, which was characterized in detail previously (Tsuru *et al*, 2009). The gene *hisC* encodes the histidinol-phosphate aminotransferase, an enzyme essential for histidine biosynthesis, and is regulated by a transcriptional attenuator in the *His* operon (Keller and Calvo, 1979; Gama-Castro *et al*, 2008). In the *hisC* rewired strain, the responsive switching of *hisC* mediated by the native transcriptional regulation of the *His* operon was unavailable. Only the stochastic switching of the engineered *hisC* monostable circuit can provide the cells a chance of survival from histidine starvation. As a result, stochastic switching-mediated adaptation was clearly observed in the *hisC* rewired strain at both population and microcolony levels. Furthermore, transcriptome analysis showed that such adaptation was associated with a global transcriptional reorganization. The stochastic switching of a monostable structure reported here strongly suggests that this stochastic strategy may represent a generic mechanism for adaptation in living organisms.

Results

The hisC rewired strain and its response to histidine depletion

The *hisC* rewired *E. coli OSU12-hisC* strain has been previously described (Kashiwagi *et al*, 2009). The gene *hisC* responsible for histidine biosynthesis was deleted from the *His* operon and placed under the control of the extraneous promoter, P_{tetA} in an engineered gene circuit inserted at a different chromosomal location (Figure 1A). Consequently, *hisC* in *OSU12-hisC* is no longer responsive to the native regulation (*His* operon) that senses histidine depletion, according to the genomic annotation around this locus. Instead, the foreign gene circuit provided a monostable structure (Supplementary Figure S1) for *hisC*'s stochastic switching. The green fluorescent protein (GFP) (*gfpuv5*) was co-expressed with *hisC* for the quantitative evaluation of HisC in single cells. The upstream regulation of TetR, whose expression level was reported by the red fluorescent protein (RFP) (*dsred.T4*), was introduced to achieve the inducible GFP (HisC) level. The full induction of TetR by isopropyl β-D-1-thiogalactopyranoside (IPTG) was applied to avoid any possible upstream noise that caused by the abundance of endogenous LacI. The doxycycline-dependent growth of *OSU12-hisC* has been characterized previously (Kashiwagi *et al*, 2009). Accordingly, the full induction of both P_{trc} and P_{tetA}, that is, the addition of 100 μM IPTG and 100 nM doxycycline, was employed here to study how the stochastic switching of *hisC* allows the cells to grow in histidine-free conditions.

Under the described condition, the response of *OSU12-hisC* to histidine depletion was examined. Cells initially grown in the presence of 1 mM histidine were inoculated into fresh medium with the same induction but without histidine. Microscopic observation clearly revealed that the cells showed stronger green fluorescence after histidine depletion (Figure 1B), which suggested an increased expression level of *hisC*. Population analysis using flow cytometry was performed to detect the difference in GFP (HisC) level of the cell populations newly formed in the presence and absence of histidine. It showed that the distributions of both GFP concentration and GFP bias (GFP/RFP ratio) in *OSU12-hisC* shifted towards a higher level in histidine-free conditions (Figure 1C and D), whereas the depletion caused only a slight change in distributions of *OSU11*, a control strain carrying both the same engineered genetic circuit and an intact *His* operon, including the *hisC* gene in its native context (Supplementary Figure S2). Repeated experiments revealed that the increases in both GFP concentration (~2.1 folds) and GFP bias (~1.5 folds) due to histidine depletion were highly significant ($P < 0.005$, $N = 6$) in *OSU12-hisC* (Supplementary Figure S3). In particular, the increased GFP bias strongly suggested that the change in gene expression occurred specifically in the rewired *hisC* (i.e., GFP) but not in all genes (e.g., RFP).

Population shift along with growth recovery and its relaxation

The temporal changes in fluorescent intensity of *OSU12-hisC* in response to histidine depletion were investigated. Exponentially growing cells in histidine-supplied conditions were transferred to fresh medium in the presence or absence of histidine, and the timed sampling was subsequently performed at 2 h intervals. *OSU12-hisC* did grow in the absence of histidine, but the growth rate was slower than that in the presence of histidine (Figure 2A). In addition, the growth of
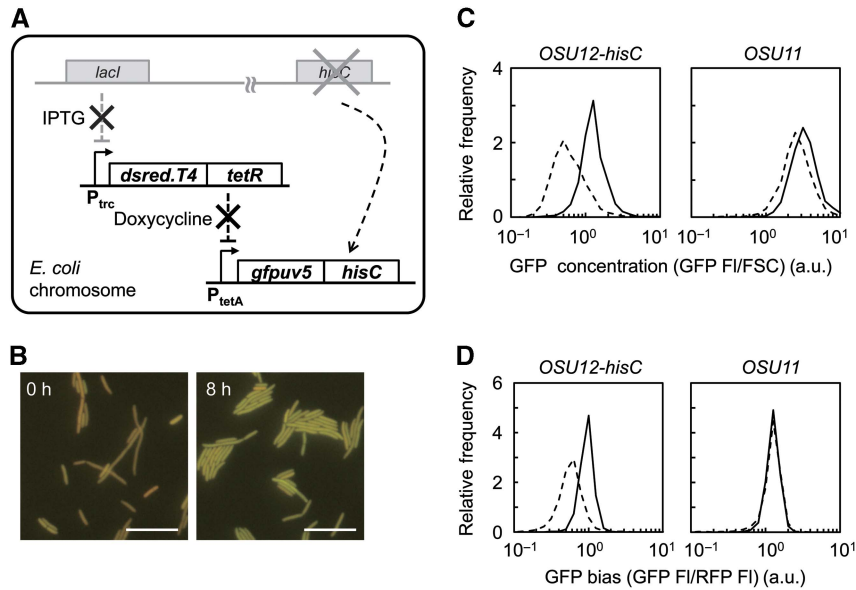
Figure 1 *OSU12-hisC* grown in the absence of histidine. (**A**) Genetic construction of *OSU12-hisC*. The gene circuit (bold fonts with dark lines) comprising the rewired *hisC* was integrated into the *E. coli* chromosome (Kashiwagi *et al*, 2009). *hisC* located in the native *His* operon was disrupted and newly controlled by the repressor TetR and the chemical doxycycline. The expression levels of TetR and RFP were regulated by the endogenous LacI and the inducer IPTG. The related genes within the inherent chromosomal locations under their native regulations are indicated in grey. (**B**) Microscopic observation of the cells before and after histidine depletion in the presence of both inducers. The scale bar represents 10 μm. (**C, D**) Steady distributions of the relative cellular GFP concentration and GFP bias in the presence (broken lines) or absence (solid lines) of histidine. *OSU11* refers to the control strain (see Supplementary Figure S2). The distributions of *OUS12-hisC* indicate the populations formed 10 or 14 h after inoculation in the presence or absence of histidine, respectively. The distributions of *OUS11* indicate the populations formed 12 or 14 h after inoculation in the presence or absence of histidine, respectively. The bin-width of the distributions is 0.1 (a.u.). Green fluorescence intensity (GFP FI), red fluorescence intensity (RFP FI) and forward scattering (FSC) represent the abundances of GFP and RFP expressed in single cells and the relative cell size, respectively. GFP FI/FSC and GFP bias (GFP FI/RFP FI) indicate the relative GFP level in cells. Source data is available for this figure at www.nature.com/msb.
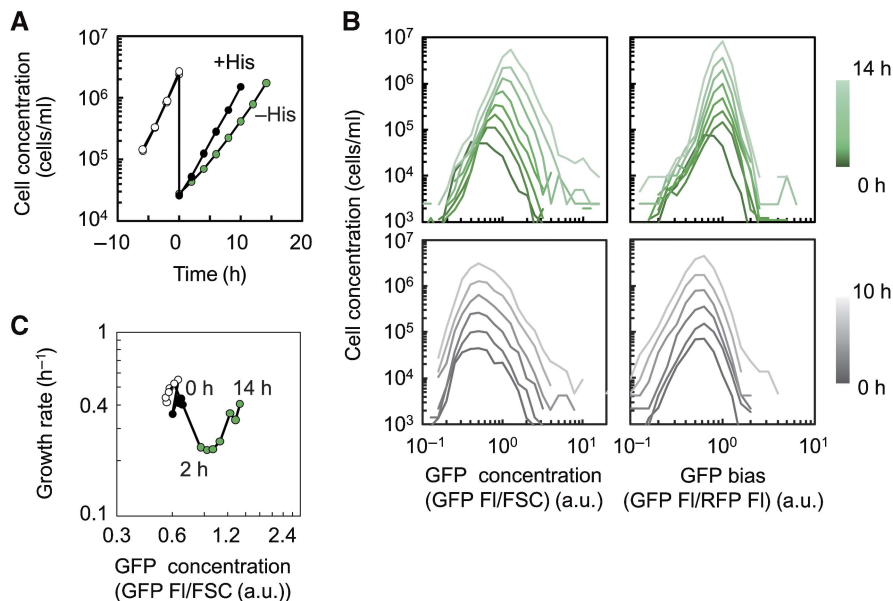

Figure 2 Temporal changes in the cell population in response to histidine depletion. (**A**) Growth curves of *OSU12-hisC* in the different nutritional conditions. Cells grown in the presence (+ His) and absence (− His) of histidine was sampled at 2 h intervals. Cycles in white, black and green refer to the cell growth before histidine depletion (pre-culture), in the presence or absence of histidine after histidine depletion, respectively. Zero hour is the time point at which histidine was removed or newly supplied. (**B**) Temporal changes in GFP level of the cell population. The distributions of GFP concentration and GFP bias in the presence (+ His) and absence (− His) of histidine are represented the cell populations in the presence (+ His) and absence (− His) of histidine, respectively. Temporal changes in the distributions are indicated for every 2 h interval as the gradation from dark to light, 0–14 h (green) and 0–12 h (grey), respectively. (**C**) Growth recovery after histidine depletion. The growth recovery trajectory is indicated with respect to the temporal change in distribution. The white, black and green cycles, and the time points are described in (A). GFP concentration and GFP bias are described in Figure 1.

OSU11 was approximately equivalent in both nutritional conditions, and the *hisC*-deleted strain, *OSU11ΔhisC* (genotype in Supplementary Figure S2), failed to propagate under conditions of starvation (Supplementary Figure S4). These results verified that the depletion of histidine did bring severe stress to the cells, due to the rewiring of the starvation-stringent gene, *hisC*.

The cell population of *OSU12-hisC* shifted gradually to higher levels of both GFP concentration and GFP bias in histidine-free conditions, but maintained the initial level in histidine-supplied conditions (Figure 2B). The cell growth rates were evaluated according to the cell concentrations between every two measurements (sampling points). Both the growth rate and the GFP level stayed approximately constant, when *OSU12-hisC* grown in the presence of histidine (Figure 2C, black cycles). On the contrary, the temporal trajectory of the relation between cell growth and GFP level showed that the growth rate dropped off markedly with histidine depletion, but recovered gradually within a few hours (Figure 2C, green cycles). In the later period, the growth rate recovered accompanied by an increase in GFP (HisC) concentration. The gradual shift along with growth recovery in response to starvation was clearly identified in the independent replications (Supplementary Figure S5). In response to external perturbations, the changes in gene expression relying on a stochastic strategy were reported to be generally slower than the changes due to operon regulation (Keller and Calvo, 1979; Zaslaver *et al*, 2004; Yamada *et al*, 2010). The slow recovery in either GFP concentration or growth rate was therefore assumed to be dependent on the stochastic switching of *hisC* located in the monostable circuit.

Furthermore, the population shift against the environmental transition showed reversibility. The cell population remained steady at the high GFP (HisC) level in the absence of histidine. However, once exponentially growing *OSU12-hisC* under starved conditions was supplied with 1 mM histidine, the population distribution returned to a low level of GFP (HisC) within 3 h (Figure 3). That is, the reduction in GFP (HisC) level of the whole population ($\sim 10^6$ cells/ml) took place within only 1–2 generations (i.e., 14–17 h). As described previously, in contrast to bistable structures, monostability did not fix the phenotype but allowed the cells to adapt dynamically.
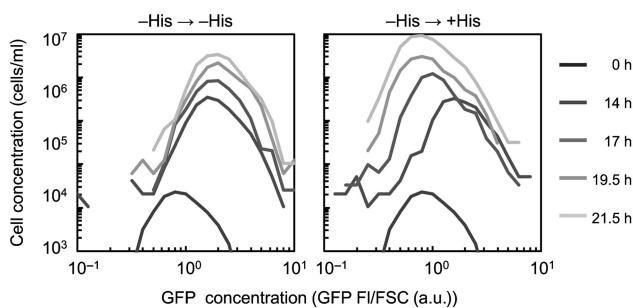

Figure 3 Reversibility of gene expression according to nutritional conditions. Changes in GFP concentration of the cell population were investigated, once *OSU12-hisC* kept growing in the absence of histidine ($-His \rightarrow -His$), or supplied with histidine 14 h after starvation ($-His \rightarrow +His$). The temporal changes in GFP concentration are shown as the distributions in greyscale from dark to light, representing the indicated sampling time points, respectively. GFP concentration is as described in Figure 1.

The relaxation to the initial steady state in response to stress release in a stochastic switching-dependent manner could only be observed only in a monostable structure. Additionally, the restoration also demonstrated that the population shift was neither caused by the mutation in genome nor due to the efficiency in GFP maturation.

Directionality in stochastic switching initiated adaptation

To examine how the stochastic switching occurring in individual cells initiated adaptation, 30–50 microcolonies were characterized in the presence or absence of histidine at time points of 0, 2 and 4 h. Cells in the logarithmic growth phase were placed on glass coverslips and covered with a thin layer of agarose gel pad medium in the presence or absence of histidine, respectively. Microcolony formation from a single cell was observed under the microscope (Figure 4A). Variation in cellular GFP level was clearly observed in individual cells (Figure 4B; Supplementary Figure S6). Stochastic switching of *hisC* was verified according to the random changes in GFP bias along with the cell division under histidine-rich conditions. For example, one of four daughter cells showing stronger green fluorescence were born from a single cell 2 h after shifting to histidine-supplied conditions, but one of seven daughter cells showed weaker green fluorescence 4 h later (Figure 4B, first row, + His). On the other hand, the microcolonies formed under the histidine-free conditions tended to higher levels of GFP bias (Figure 4B; Supplementary Figure S6). For example, two daughter cells of higher GFP bias appeared 2 h after histidine depletion; subsequently, four daughter cells with stronger or similar GFP level were born (Figure 4B, first row, −His). The directional tendency favoured the high GFP (HisC) level, which was evidently detected in the first 2 h after histidine depletion, resulting in a population shift (Figure 4C). In contrast, the distributions of microcolonies grown in histidine-supplied conditions kept steady, due to the randomized directions of stochastic switching (Figure 4C). In addition, the restoration to lower GFP bias upon addition of histidine (i.e., stress release) was clearly observed at the microcolony level as well (Supplementary Figure S7). Such dynamic changes in microcolonies were consistent with the population dynamics (Figures 2 and 3).

As the preferential direction was evident from 0 to 2 h (weaker after 2 h) (Figure 4; Supplementary Figure S8), the initial cellular status that shaped the subsequent adaptation was further analysed. GFP bias and growth rates were initially partially correlated (~ 0.51, $P < 0.05$) for microcolonies growing in the absence of histidine. In comparison, those growing in the presence of histidine showed no correlation (Figure 5A). This observation suggested that the initial state may have a role in determining, to some extent, the growth rate. Moreover, a weak positive correlation (~ 0.52, $P < 0.01$) was found between the initial GFP bias and the subsequent changes in cellular status (i.e., relative change in GFP bias) only in histidine-free conditions (Figure 5B). In particular, under starved conditions, higher initial GFP bias and larger relative changes were detected in the growing cells than in the non-growing cells. Taken together, these results indicated that
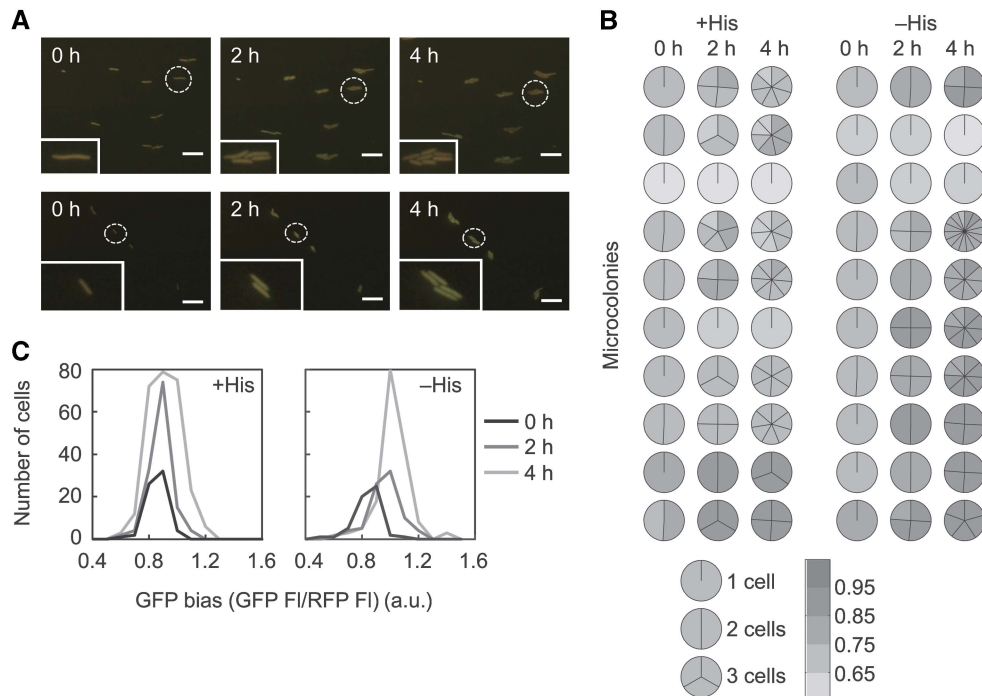
Figure 4 Time trace of cells at the microcolony level. (**A**) Snapshot of the cells grown under the microscope in the presence (upper panel) or absence (bottom panel) of histidine at 0, 2 and 4 h. The insets show higher magnification views of the microcolonies indicated by broken lines. The scale bar represents 10 μm. (**B**) Temporal changes in cell number and GFP bias of the microcolonies in the presence (+His) or absence (−His) of histidine. The divisions in the circle represent the numbers of cells grown in a single microcolony, and the gradation (greyscale) from light to dark represents the GFP bias. (**C**) Distributions of GFP bias at the single-cell level within the microcolonies grown in the presence (+His) or absence (−His) of histidine. From 30 to 50 microcolonies in each condition were used for population analysis (10 microcolonies are shown here, and the others are shown in Supplementary Figure S6). Greyscale from dark to light represents the sampling time points at 0, 2 and 4 h, respectively.

the stochastic fluctuations in the initial state had an important role not only in fate decision (i.e., whether to grow) but also in the directionality of the stochastic switch. Note that the unfit cells not only depended on the initial GFP level but are also born stochastically from the growing fit microcolonies (Supplementary Figure S9).

Transcriptional reorganization for adaptation

As the changes in expression of a single gene, *hisC*, are generally insufficient for the cells to survive to histidine starvation, transcriptome analysis was additionally performed to investigate global alterations in gene expression in the *OSU12-hisC* strain. Cells exponentially growing in the presence or absence of histidine were collected for microarray profiling. The steady expression pattern of *OSU12-hisC* was close to that of *OSU11* in the presence of histidine, but different in the absence of histidine, according to the scatter plot of total 4467 genes (Figure 6A). A considerably larger number of genes up- or downregulated in response to histidine depletion was observed in *OSU12-hisC* than in *OUS11*, and the majority of these genes did not overlap between the two strains (Figure 6B). In total, 225 and 200 genes that were specifically upregulated or downregulated in *OSU12-hisC*, respectively, were further characterized according to their categories as previously reported (Riley *et al*, 2006). The genes in the categories of RNA (n), structural component (s) and transporter (t) were mostly downregulated (Table I). The genes encoding tRNAs, ribosomal proteins and fimbrial proteins
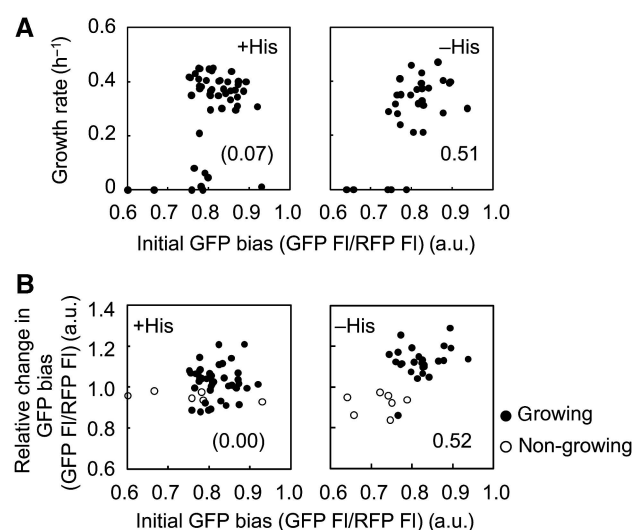

Figure 5 Relations among cell growth, initial state and cellular reactivity. Individual cells in the microcolonies (from 0 to 2 h) grown in the presence (+His) or absence (−His) of histidine were analysed. (**A**) Relationship between cell growth rate and initial GFP bias. The growth rate was calculated using the pixel numbers of the total area of each microcolony. The initial GFP bias is the ratio between GFP Fl and RFP Fl of the total area of each microcolony at 0 h. Spearman's rank correlation coefficients are indicated as 0.51 ($P < 0.05$) and 0.07 ($P > 0.1$). (**B**) Relationship between cellular reactivity and initial GFP bias. Relative change in GFP bias represents the cellular reactivity, and is the ratio between the GFP bias 2 h after histidine depletion and the initial GFP bias. Individual cells in the microcolonies were divided into growing (closed circles) and non-growing (open circles). Spearman's rank correlation coefficients are indicated as 0.00 ($P > 0.1$) and 0.52 ($P < 0.01$). Source data is available for this figure at www.nature.com/msb.
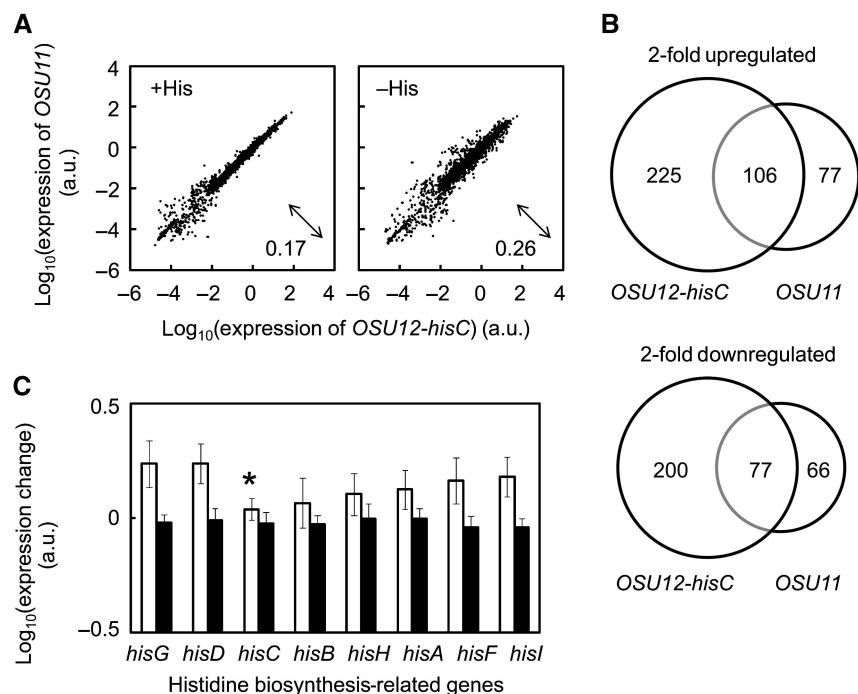
Figure 6 Transcriptional changes. (**A**) Correlation of expression between *OSU11* and *OSU12-hisC*. The relative mRNA level in the presence (+His) or absence (−His) of histidine was calculated as the averaged value of three independent experiments. Standard deviations are indicated. (**B**) Venn diagrams of the numbers of upregulated and downregulated genes due to histidine depletion. The numbers in each area correspond to the numbers of genes. (**C**) Transcriptional changes of genes related to histidine biosynthesis. The ratio of mRNA concentration between (+His) and (−His) in *OSU12-hisC* and *OSU11* are shown as open and closed bars, respectively. Error bars represent the standard deviation of three independent experiments. Asterisk indicates the difference in chromosomal location. Source data is available for this figure at www.nature.com/msb.

Table I Significant upregulated and downregulated gene categories

Categories	Categories	Number of total genes	Number of upregulated genes	*P*-value	Number of downregulated genes	*P*-value
Carrier	c	77	9	0.015	1	0.97
Cell process	cp	56	2	0.78	0	1.0
Partial information	d	147	10	0.21	3	0.96
Enzyme	e	1092	33	~1.0	52	0.34
Factor	f	149	15	0.0085	1	~1.0
Phage/IS in common	h	311	25	0.015	10	0.89
Leader peptide	l	11	0	1.0	3	0.011
Lipoprotein	lp	46	2	0.68	2	0.62
Membrane	m	43	0	1.0	2	0.58
RNA	n	127	5	0.77	21	2.4×10^{-7}
Unknown function	o	472	40	0.0011	7	~1.0
Carrier, predicted	pc	42	0	1.0	0	1.0
Enzyme, predicted	pe	390	12	0.98	8	~1.0
Factor, predicted	pf	61	10	0.00089	3	0.52
Phase/IS in common, predicted	ph	10	0	1.0	0	1.0
Membrane, predicted	pm	211	16	0.069	7	0.84
Regulator, predicted	pr	164	6	0.84	2	~1.0
Structural component, predicted	ps	37	6	0.0099	1	0.82
Transporter, predicted	pt	254	12	0.63	13	0.35
Regulator	r	242	6	0.98	11	0.52
Structural component	s	88	0	1.0	10	0.006
Pseudogenes in common	su	94	9	0.048	8	0.06
Transporter	t	343	7	~1.0	35	6.6×10^{-6}
	Total	4467	225		200	

OSU12-hisC specific upregulated and downregulated genes (shown in Figure 5) were divided into 23 categories, according to the previous report (Riley *et al*, 2006). One-tailed *t*-test (*P*<0.01) was performed to determine significance. The expression profiles of the total 12 data sets are provided (Supplementary Table S1).

were found in these categories, for example, reduced swimming caused by repressed translation as an energy-saving tactic, which is known as a stringent response (Srivatsan and Wang, 2008; Traxler *et al*, 2008). The upregulated genes were significantly clustered in the categories of factors (f and pf), unknown function (o) and predicted structural component (ps).

These observations strongly suggested that diverse adaptive cellular states were achieved both by the responsive switching that relied on operon regulation and by the stochastic switching of the rewired gene.

In addition, the transcriptional changes of the structural genes in the *His* operon were greater in *OSU12-hisC* than in *OSU11* (Figure 6C; Supplementary Figure S10). In particular, *hisG* and *hisD*, located downstream of the promoter, were significantly induced. The levels of expression of genes downstream of the native *hisC* locus (*hisB–hisI*) increased as well, in a location-dependent manner. The enhanced expression of these genes probably compensated for the perturbed native regulation and facilitated sufficient production of histidine. We assume that the transcriptional reorganization improved the expression levels of multiple genes crucial for growth recovery in a synchronized manner with the occasionally increased *hisC* expression.

Discussion

Bistable structures are considered as evolved designs for adaptation (Acar *et al*, 2008), whereas monostability relies on a simpler design, which is much more common in regulatory networks (Newman *et al*, 2006; Taniguchi *et al*, 2010). In this study, we showed that adaptation to starvation can be successfully achieved by stochastic switching of *hisC* under a monostable control (Figure 2). The results showed that the cell population remained at an unstable but adaptive state under starved conditions, but returned to the original stable state once histidine was supplied (Figure 3). It indicated that the selective proliferation of fit cells was sufficiently high to compensate the relaxation of the monostable control structure to the stable but unfit state. This probably resulted from comparable time scales of both the stochastic changes in protein level and the cell growth rate, in accordance with the theoretical proposal that an adaptive state can be fixed by biased growth (i.e., the balance of frequency in protein fluctuation with generation time) in a monostable structure (Sato and Kaneko, 2006). In summary, the present study provides experimental evidence that stochastic switching can contribute to adaptation without a complex responsive or bistable design.

In contrast to previous gene rewiring studies using native regulation (Stolovicki *et al*, 2006; Stern *et al*, 2007; Isalan *et al*, 2008), a foreign regulation strategy was adopted here, to minimize disturbances from the native regulatory system. An inducible cascade circuit was employed here to taken into account stochastic noise in gene expression, which depends markedly on the gene function and its regulation (Newman *et al*, 2006; Taniguchi *et al*, 2010). This genetic structure has been previously widely used (Pedraza and van Oudenaarden, 2005; Rosenfeld *et al*, 2005; Kashiwagi *et al*, 2009; Tsuru *et al*, 2009), and its monostability and stochasticity were clearly characterized by varying the concentrations of inducers (Pedraza and van Oudenaarden, 2005; Rosenfeld *et al*, 2005; Tsuru *et al*, 2009). Under induced conditions, a gradual change in both GFP concentration and GFP bias was observed together with a unimodal distribution characteristic of a monostable structure (Pedraza and van Oudenaarden, 2005; Rosenfeld

et al, 2005; Tsuru *et al*, 2009). In the present study, the full induction of TetR (i.e., addition of 100 nM doxycycline) was used to break the cascaded structure. The stochastic expression of *hisC* was only due to the promoter P_{tetA} without any upstream contribution, as the full induction avoided amplification of the noise in the upstream promoters, that is, both the foreign P_{trc} and the endogenous P_{lacI}.

As the cascaded gene circuit comprised both GFP and RFP, it was used as a two-colour system to identify the specific changes in GFP (HisC) level according to the ratio between GFP and RFP (i.e., GFP bias). The addition of 100 μM IPTG not only masked the intrinsic LacI to maximize the TetR level, but also intensified the red fluorescence to reach a steady RFP level, which facilitated the precise estimation of GFP bias. In contrast to the GFP concentration (GFP/FS) that maintained approximately steady independent on IPTG, the GFP bias increased considerably due to the absence of IPTG (Supplementary Figure S11). Nevertheless, the shift of the *OSU12-hisC* population to higher GFP (HisC) levels in response to histidine depletion was independent of the addition of IPTG (Supplementary Figure S11). Additionally, the steady distributions of *OSU12-hisC* and *OSU11* were quite different in GFP levels even under the same inductions (Figure 1C and D; Supplementary Figures S3 and S11). Actually, it remains unclear why gene expression levels changed even under identical regulation, an observation which was reported previously as well (Stolovicki *et al*, 2006; Stern *et al*, 2007; Isalan *et al*, 2008). The increase in GFP (HisC) levels in response to starvation occurred in *OSU12-hisC* but not in *OSU11*, in spite of the fact that both strains had reached their maximal levels of GFP (HisC) before histidine depletion. In conclusion, the increase in GFP (HisC) was a phenomenon unique to the adaptation of the engineered *OSU12-hisC* strain.

We propose that the adaptation of *OSU12-hisC* consists of two scenarios: (1) the directional response of individual cells towards high level of HisC was initiated in the early period (0–2 h); (2) rapid growth of stochastically appearing cells with high HisC level overtook the population in the late period (after 2 h). These scenarios were also supported by the population dynamics (Figure 2). For instance, in the initial period of adaptation (0–2 h), the population increase, which represents both the growth of the cells with fixed expression level and the transition of the cells from other expression levels, dropped to negative at low GFP level, but increased markedly at high GFP level (Supplementary Figure S12). It suggested that cells with low GFP level switched high GFP levels and accelerated the population shift. In addition, the population increase remained constant independent on GFP concentration in the presence of histidine, but largely varied in the absence of histidine (Supplementary Figure S12). It indicated that only cells with high GFP (HisC) level could proliferate.

Moreover, the transcriptome analysis showed that a large number of genes were involved in the stochastic switching-induced adaptation (Figure 6). The global transcriptional change must be driven somewhat directionally; otherwise an extremely long time would be required for all of these genes to reach the appropriate state in a stochastic manner. Such directionality was suggested by the stochastic switching of *hisC* in response to starvation (Figure 4). Since adaptation by

stochastic switching is initiated by the proliferation of a very small number of occasionally appearing fit cells, the process tends to be slow (Koch, 1988; Nguyen *et al*, 1989; Dong *et al*, 1995; Kussell and Leibler, 2005). The directionality observed here may have had a role in increasing the initial number of fit cells and improved the efficiency of stochastic switching-mediated adaptation. It may also result from evolving mechanisms that are intermediate between stochastic switching and signal-dependent regulation. Regulatory mechanisms that respond to a specific environmental condition, for example, signal transduction, may be a consequence of evolutionary canalization (Waddington, 1959; Eldar *et al*, 2009; Raj *et al*, 2010) and eventual fixation of the primitive multireactivity of heterogeneous cell populations, once such conditions become frequent.

Materials and methods

Strains

The *E. coli* strains *OSU11*, *OSU11ΔhisC* and *OSU12-hisC* (Supplementary Figure S2) were described previously (Kashiwagi *et al*, 2009). These strains commonly carry a core gene circuit, P_{tetA}–*gfpuv5* and P_{trc}–*dsred.t4-tetR–PEM7–zeo*, on the genome, located at *galK* and *intC* sites, respectively. P_{tetA}–*gfpuv5* consists of the promoter P_{tetA} and the mutated *gfp* gene (*gfpuv5*) encoding the GFP, and P_{trc}–*dsred.t4–tetR–PEM7–zeo* is comprising the promoter P_{trc}, *dsred.t4* encoding RFP, *tetR* encoding the repressor protein, and the independent expression unit of the Zeocin resistance gene, *zeo*, with its promoter PEM7. *OSU11ΔhisC* is the *hisC* knockout mutant of *OSU11* carrying the rewired *hisC* gene downstream of *gfpuv5*.

Cell culture

E. coli cells were grown in minimal medium, modified M63 (mM63: 62 mM K_2HPO_4, 39 mM KH_2PO_4, 15 mM $(NH_4)_2SO_4$, 2 μM FeS-$O_4 \cdot 7H_2O$, 15 μM thiamine hydrochloride, 203 μM $MgSO_4 \cdot 7H_2O$ and 22 mM glucose) (Kashiwagi *et al*, 2009) in the presence or absence of 1 mM histidine. *OSU12-hisC* was grown in mM63 medium supplied with 25 μg/ml kanamycin and 1 mM histidine. Cells were cultured at 37°C for several passages until the growth rate became stable. Full expression of RFP was induced in the presence of 100 μM isopropyl IPTG. Exponentially growing cells were subsequently transferred to fresh medium supplemented with 100 nM doxycycline hydrochloride (Dox) to induce the expression of GFP. The initial cell concentration was ~10^4 cells/ml.

Nutrient depletion

Bacterial cells were grown in mM63 medium supplemented with 25 μg/ml kanamycin, 1 mM histidine, 100 μM IPTG and 100 nM Dox for 18 h as described above. Aliquots of 300 μl of exponentially growing cells (about 10^6 cells/ml) were harvested by centrifugation at 5000 r.p.m. (or 2300 g) for 30 s at 37°C using spin columns (Ultrafree-MC Centrifugal Filter Units, 0.2 μm; Millipore). After discarding the flow-through fraction, the cells were washed with 300 μl of the same medium minus histidine. After repeating centrifugation and washing processes twice, the concentration of the cell suspension was measured by flow cytometry and inoculated into 5 ml of the same medium without histidine, where the initial cell concentration was ~10^4 cells/ml.

Flow cytometry

Gene expression (fluorescence intensity) and cell volume were evaluated using a flow cytometer (FACSAria cell sorter; Becton Dickinson) with a 488-nm argon laser, a 515–545 nm emission filter (GFP) and a 563–589 nm emission filter (RFP). The following PMT voltage settings were applied: forward scatter (FSC), 203; side scatter (SSC), 440; GFP, 615; and RFP, 593. The flow data were converted to TXT format. The cellular GFP concentration was calculated by dividing the green fluorescence value by the FSC value using MATLAB (The MathWorks Inc.), as described previously (Tsuru *et al*, 2009). Autofluorescence was subtracted. Systematic errors resulting from events that occurred at the bottom or top of the instrument's range were eliminated. Data from 1000 to 10 000 cells were collected for each measurement. Cell samples mixed with fluorescent beads (Floresbrite YG Microspheres, 2 μm; Polysciences Inc.) were loaded for calculation of cell concentration.

Microscopic observation and image acquisition

OSU12-hisC was grown overnight in mM63 medium supplemented with 25 μg/ml kanamycin, 1 mM histidine, 100 μM IPTG and 100 nM Dox, at 37°C. Cells (4 μl of cell culture) in the logarithmic growth phase were placed on glass coverslips and covered with a thin layer of agarose gel (1.5%) pad medium containing 25 μg/ml kanamycin, 100 μM IPTG and 100 nM Dox, with or without 1 mM histidine. The cover glasses with the inoculated cells were incubated at 37°C and observed every 2 h. The fluorescence images were acquired using a fluorescence microscope (IX70; Olympus) and recorded using a CCD camera (VB-6010; Keyence).

Image analysis

Time series images of the green and red fluorescence were used to analyse the fluorescence (green for GFP FI and red for RFP FI) and shape of cells. Phase contrast images were used for identification and segregation of cells. Shapes of camera-captured cells were outlined using ImageJ (http://rsbweb.nih.gov/ij/) automatically and manually, respectively. The area of cells was calculated by summing the number of fluorescent pixels. Growth rates were determined by an exponential fit to the cells' area over sampling time intervals. Green and red fluorescence of each microcolony or each cell were determined by averaging pixel intensity. GFP bias (GFP FI/RFP FI) was calculated by dividing green fluorescence by red fluorescence. The relative change in GFP bias was calculated over sampling time intervals, and 30–50 microcolonies (up to ~270 cells) were measured.

Sample preparation and microarray

Exponential cell growth was interrupted by putting the cell culture into cold phenol–ethanol solution (1 g of phenol in 10 ml of ethanol) prepared in advance. The cells were collected by centrifugation at 16 000 g for 5 min at 4°C, and the pelleted cells were stored at −80°C before use. Total RNAs were extracted using an RNeasy mini kit (Qiagen) in accordance with the manufacturer's instructions. The quantity of the purified RNA was carefully determined by the absorbance at 260 nm using a NanoDrop ND-1000 (Thermo Fisher Scientific Inc.), an Agilent 2100 Bioanalyzer with an RNA 600 Nano kit (Agilent Technologies) and electrophoresis on an agarose gel under reducing conditions. High-density oligonucleotide microarray gene expression analysis was performed using an Affymetrix GeneChip system. The cDNA synthesis, fragmentation, labelling and hybridization of cDNA were carried out according to the Affymetrix GeneChip Expression Analysis Technical Manual. To improve the efficiency of labelling, the incubation time was increased to 2 h. Three to five independent experiments (sample preparations) were performed for each condition.

Array design

A high-density DNA microarray (Suzuki *et al*, 2007; Ono *et al*, 2008) covering the whole genome of *E. coli* W3110 strain (GenoBase; http://ecoli.naist.jp/GB6/search.jsp) was utilized. Both strands of the genome were alternately tiled at single-base resolution using 21-mer perfectly matching and three mismatching probes. A library consisting

of a total of 18.6 million probes was arranged on three GeneChips for microarray analysis, covering four types of probe throughout the 4.6-Mb *E. coli* genome. One of three GeneChips was used here for transcriptional analysis.

Data extraction and analysis

Microarray data were extracted using custom scripts written in R (Ihaka and Gentleman, 1996) based on the finite hybridization model (Ono *et al*, 2008) and the thermodynamic model of non-specific binding on short nucleotide microarrays (Furusawa *et al*, 2009). Three data sets from 3 to 5 repeated microarray assays were used for mRNA profiling analysis. To avoid any significant error due to the diverse signal intensities in GeneChips, the array results only showing the identical distribution of probe fluorescence intensity were subjected to subsequent expression analysis. A total of 12 array results for two strains under two conditions (in triplicate) were finally used. The microarray raw data sets have been deposited in NCBI's Gene Expression Omnibus and are accessible through GEO Series accession number GSE28210 (http://www.ncbi.nlm.nih.gov/geo/query/acc.cgi?acc=GSE28210). In all, 4467 genes were used for the analysis and global normalization was performed for 12 data sets of mRNA transcriptional level. The gene names and the gene categories are based on the genome information of W3110 and the genes in common to strains W3110 and MG1655 (Riley *et al*, 2006). The whole data set of gene names and categories is from GenoBase, Japan (http://ecoli.naist.jp/gb6/Download.html).

Supplementary information

Supplementary information is available at the *Molecular Systems Biology* website (www.nature.com/msb).

Acknowledgements

Conflict of interest

The authors declare that they have no conflict of interest.

References

Acar M, Mettetal JT, van Oudenaarden A (2008) Stochastic switching as a survival strategy in fluctuating environments. *Nat Genet* **40:** 471–475

Avery SV (2006) Microbial cell individuality and the underlying sources of heterogeneity. *Nat Rev Microbiol* **4:** 577–587

Balaban NQ, Merrin J, Chait R, Kowalik L, Leibler S (2004) Bacterial persistence as a phenotypic switch. *Science* **305:** 1622–1625

Carroll SB (2005) Evolution at two levels: on genes and form. *PLoS Biol* **3:** e245

Crombach A, Hogeweg P (2008) Evolution of evolvability in gene regulatory networks. *PLoS Comput Biol* **4:** e1000112

Dong H, Nilsson L, Kurland CG (1995) Gratuitous overexpression of genes in Escherichia coli leads to growth inhibition and ribosome destruction. *J Bacteriol* **177:** 1497–1504

Eldar A, Chary VK, Xenopoulos P, Fontes ME, Loson OC, Dworkin J, Piggot PJ, Elowitz MB (2009) Partial penetrance facilitates developmental evolution in bacteria. *Nature* **460:** 510–514

Furusawa C, Ono N, Suzuki S, Agata T, Shimizu H, Yomo T (2009) Model-based analysis of non-specific binding for background correction of high-density oligonucleotide microarrays. *Bioinformatics* **25:** 36–41

Gama-Castro S, Jimenez-Jacinto V, Peralta-Gil M, Santos-Zavaleta A, Penaloza-Spinola MI, Contreras-Moreira B, Segura-Salazar J, Muniz-Rascado L, Martinez-Flores I, Salgado H, Bonavides-Martinez C, Abreu-Goodger C, Rodriguez-Penagos C, Miranda-Rios J, Morett E, Merino E, Huerta AM, Trevino-Quintanilla L, Collado-Vides J (2008) RegulonDB (version 6.0): gene regulation model of Escherichia coli K-12 beyond transcription, active (experimental) annotated promoters and Textpresso navigation. *Nucleic Acids Res* **36:** D120–D124

Henkin TM, Yanofsky C (2002) Regulation by transcription attenuation in bacteria: how RNA provides instructions for transcription termination/antitermination decisions. *Bioessays* **24:** 700–707

Ihaka R, Gentleman R (1996) R: a language for data analysis and graphics. *J Comput Graph Stat* **5:** 299–314

Isalan M, Lemerle C, Michalodimitrakis K, Horn C, Beltrao P, Raineri E, Garriga-Canut M, Serrano L (2008) Evolvability and hierarchy in rewired bacterial gene networks. *Nature* **452:** 840–845

Jacob F, Monod J (1961) Genetic regulatory mechanisms in the synthesis of proteins. *J Mol Biol* **3:** 318–356

Kashiwagi A, Sakurai T, Tsuru S, Ying BW, Mori K, Yomo T (2009) Construction of Escherichia coli gene expression level perturbation collection. *Metab Eng* **11:** 56–63

Kashiwagi A, Urabe I, Kaneko K, Yomo T (2006) Adaptive response of a gene network to environmental changes by fitness-induced attractor selection. *PLoS One* **1:** e49

Keller EB, Calvo JM (1979) Alternative secondary structures of leader RNAs and the regulation of the trp, phe, his, thr, and leu operons. *Proc Natl Acad Sci USA* **76:** 6186–6190

Koch AL (1988) Why can't a cell grow infinitely fast? *Can J Microbiol* **34:** 421–426

Kussell E, Leibler S (2005) Phenotypic diversity, population growth, and information in fluctuating environments. *Science* **309:** 2075–2078

Newman JR, Ghaemmaghami S, Ihmels J, Breslow DK, Noble M, DeRisi JL, Weissman JS (2006) Single-cell proteomic analysis of S. cerevisiae reveals the architecture of biological noise. *Nature* **441:** 840–846

Nguyen TN, Phan QG, Duong LP, Bertrand KP, Lenski RE (1989) Effects of carriage and expression of the Tn10 tetracycline-resistance operon on the fitness of Escherichia coli K12. *Mol Biol Evol* **6:** 213–225

Ono N, Suzuki S, Furusawa C, Agata T, Kashiwagi A, Shimizu H, Yomo T (2008) An improved physico-chemical model of hybridization on high-density oligonucleotide microarrays. *Bioinformatics* **24:** 1278–1285

Pedraza JM, van Oudenaarden A (2005) Noise propagation in gene networks. *Science* **307:** 1965–1969

Raj A, Rifkin SA, Andersen E, van Oudenaarden A (2010) Variability in gene expression underlies incomplete penetrance. *Nature* **463:** 913–918

Riley M, Abe T, Arnaud MB, Berlyn MK, Blattner FR, Chaudhuri RR, Glasner JD, Horiuchi T, Keseler IM, Kosuge T, Mori H, Perna NT, Plunkett III G, Rudd KE, Serres MH, Thomas GH, Thomson NR, Wishart D, Wanner BL (2006) Escherichia coli K-12: a cooperatively developed annotation snapshot—2005. *Nucleic Acids Res* **34:** 1–9

Rosenfeld N, Young JW, Alon U, Swain PS, Elowitz MB (2005) Gene regulation at the single-cell level. *Science* **307:** 1962–1965

Sato K, Kaneko K (2006) On the distribution of state values of reproducing cells. *Phys Biol* **3:** 74–82

Slatkin M (1974) Cascading speciation. *Nature* **252:** 701–702

Srivatsan A, Wang JD (2008) Control of bacterial transcription, translation and replication by (p)ppGpp. *Curr Opin Microbiol* **11:** 100–105

Stern S, Dror T, Stolovicki E, Brenner N, Braun E (2007) Genome-wide transcriptional plasticity underlies cellular adaptation to novel challenge. *Mol Syst Biol* **3:** 106

Stolovicki E, Dror T, Brenner N, Braun E (2006) Synthetic gene recruitment reveals adaptive reprogramming of gene regulation in yeast. *Genetics* **173:** 75–85

Suel GM, Kulkarni RP, Dworkin J, Garcia-Ojalvo J, Elowitz MB (2007) Tunability and noise dependence in differentiation dynamics. *Science* **315:** 1716–1719

Suzuki S, Ono N, Furusawa C, Kashiwagi A, Yomo T (2007) Experimental optimization of probe length to increase the sequence specificity of high-density oligonucleotide microarrays. *BMC Genomics* **8:** 373

Suzuki T, Kashiwagi A, Urabe I, Yomo T (2006) Inherent characteristics of gene expression for buffering environmental changes without the corresponding transcriptional regulations. *Biophysics* **2:** 63–70

Taniguchi Y, Choi PJ, Li GW, Chen H, Babu M, Hearn J, Emili A, Xie XS (2010) Quantifying E. coli proteome and transcriptome with single-molecule sensitivity in single cells. *Science* **329:** 533–538

Traxler MF, Summers SM, Nguyen HT, Zacharia VM, Hightower GA, Smith JT, Conway T (2008) The global, ppGpp-mediated stringent response to amino acid starvation in Escherichia coli. *Mol Microbiol* **68:** 1128–1148

Tsuru S, Ichinose J, Kashiwagi A, Ying BW, Kaneko K, Yomo T (2009) Noisy cell growth rate leads to fluctuating protein concentration in bacteria. *Phys Biol* **6:** 036015

Waddington CH (1959) Canalization of development and genetic assimilation of acquired characters. *Nature* **183:** 1654–1655

Yamada T, Ou J, Furusawa C, Hirasawa T, Yomo T, Shimizu H (2010) Relationship between noise characteristics in protein expressions and regulatory structures of amino acid biosynthesis pathways. *IET Syst Biol* **4:** 82–89

Zaslaver A, Mayo AE, Rosenberg R, Bashkin P, Sberro H, Tsalyuk M, Surette MG, Alon U (2004) Just-in-time transcription program in metabolic pathways. *Nat Genet* **36:** 486–491